In-line PIV Using a Schlieren System

M. Raffel[1*], A. Heintz[1], J.N. Braukmann[1], C.C. Wolf[1] and J.T. Heineck[2]
1: Institute of Aerodynamics and Flow Technology, German Aerospace Center (DLR), 37073 Göttingen, Germany
2: Experimental Aero-physics Branch, NASA Ames Research Center, Moffett Field, CA, 94035, USA
* Correspondent author: Markus.Raffel@dlr.de

Keywords: PIV recording, In-Line PIV, Forward scattering, Schlieren system

ABSTRACT

The article describes recent tests and developments of PIV recording and evaluation techniques that take advantage of strong forward scattering of tracer particles by in-line recording set ups. By collimating the light of a low-power light source between a pair of schlieren mirrors the observation area is increased to more than 350 mm. The same setup allows for schlieren recording of density gradients.

1. Introduction

Since the obtained particle image intensity and the contrast of PIV recordings is directly proportional to the scattered light power, it is often more effective and economical to increase the image intensity by properly choosing the scattering particles instead of increasing the laser power. In general, the light scattered by small particles is a function of the particle's size, shape, orientation and the ratio of the refractive indices of the particles and the surrounding medium. Furthermore, the light scattering depends on polarization and observation angle. For spherical particles with diameters larger than the wavelength of the incident light, Mie's scattering theory can be applied. A detailed description and discussion are given in the literature (Adrian 1991, Bohren and Huffman 1998, Raffel 2018).

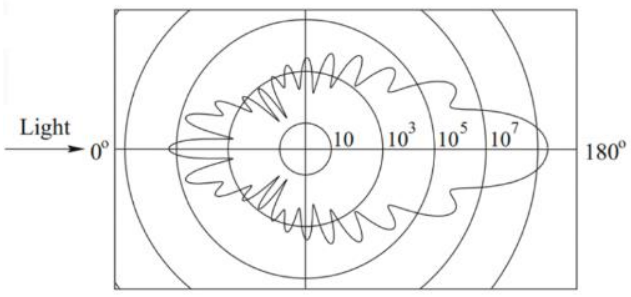

Fig. 1 Relative light scattering intensity of an oil particle of 1 µm diameter in air (Raffel 2018)

Figure 1 shows the polar distribution of the scattered light intensity for oil particles of 1 µm diameter in air with a wavelength of 532 nm according to Mie's theory. The intensity is shown on a logarithmic scale, and the circular isolines were chosen to differ by a factor of 100.

The current work demonstrates the feasibility of two in-line imaging configurations and the subsequent evaluation (see Fig. 2) and extends on parallel work presented in (Raffel et al. 2024). When the camera is placed in-line, the effective measurement volume depth in the direction of the line of sight is not limited by the well-defined edges of a laser light sheet or volume, but by the depth of focus (DoF) of the camera/lens combination as defined by Naumann and Schröder (1992). The most commonly used optical in-line measurement technique in aerodynamics is schlieren or shadow photography (Schardin 1934, 1942). The optical setup of Toepler's schlieren method consists of spherical mirrors or lenses and a light trap, often in the form of a half aperture, e.g. a knife edge. It captures variations in light intensity proportional to the first derivative of the fluid density (Settles 2001). However, setups used for schlieren photography can also be used for in-line PIV. A setup very similar to Toepler's schlieren method was implemented within this study and is described further below.

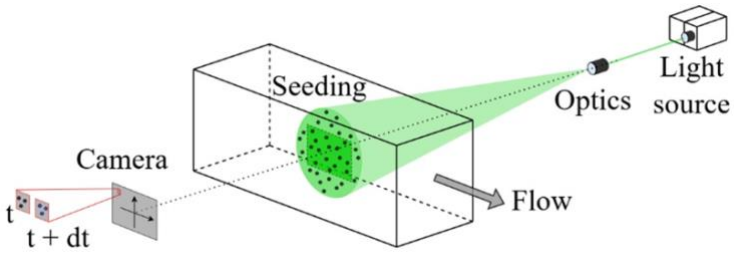

Fig. 2 Sketch of a sample setup for in-line PIV.

2. Optical setup for in-line PIV recording by large aperture schlieren mirrors

Figure 3 depicts an example of an improved in-line PIV set up using two schlieren mirrors of 400 mm diameter and 4000 mm focal length. The laser light is focused by the two large focusing mirrors onto a light trap, which is located in front of a distant imaging lens. With the exception of smaller quantities due to lens imperfections and pollutions, the majority of the emitted light is hindered from reaching the imaging sensor. Here the image is subject to the imperfections of both mirrors. On the other hand, this configuration allows for a wider field of view, with a constant illumination diameter along the measurement volume. In the first sample case, the ejector nozzle (D=100 mm)

of a seeding generator was placed in the measurement volume, with the generator providing both flow tracers and a constant low-speed airflow crossing the field of view in upward direction. The second application of the in-line PIV technique describes the measurement of a cylinder wake flow in a wind tunnel utilizing the same tracer particles illuminated with pulsed LED light. More conventional tracer particles based on atomized DEHS have been used in order to measure the cylinder wake as described in the last paragraph. Those micron sized particles required the illumination by an intermittently working cw-laser of 5.2 W maximum power.

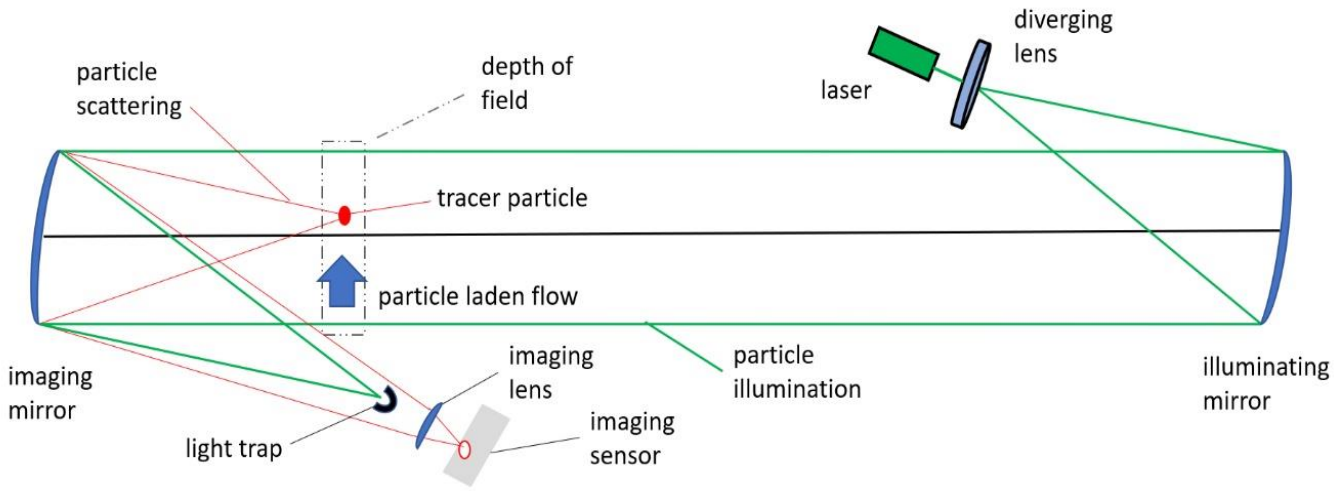

Fig. 3 Example setup for in-line PIV recording with schlieren mirrors and light trap between the receiving imaging mirror and the imaging lens.

In contrast to conventional light-sheet based PIV, in-line PIV is expected to have an increased image background intensity level caused by lens imperfections, lens contamination and out-of-focus tracer particles. The light scattered by particles within the depth of field of the imaging lens is well concentrated on a few pixels and can therefore be enhanced by digital image filtering.

3. Water droplet seeding and low power CW laser illumination

In case of the experiment described first, the light of a low-cost diode-pumped solid-state laser (Spectra Physics Excelsior, λ=532 nm, P(cont.) = 0.25 W) is expanded to about 400 mm over a distance of 4 m using a set of two biconcave lenses. The illuminated volume is imaged by a high-speed CMOS camera (PCO.Dimax S4) with an acquisition rate of 1.2 kHz, an image exposure time 19 µs, and a resolution of 2016x2016 px. It has been fitted with an f = 300 mm macro lens (Nikon AF-S Nikkor 55-300 mm). The image lens working distance is 2015 mm between the lens and the imaging mirror plus an additional 2000 mm between the mirror and the plane of focus. With the

lens aperture set to f# = 5.6, the DoF is estimated at 25 mm. A series of 500 images was recorded within 0.41 seconds. Water droplets with a diameter of about D_p = 2 − 3 µm were provided by a custom-built DLR generator.

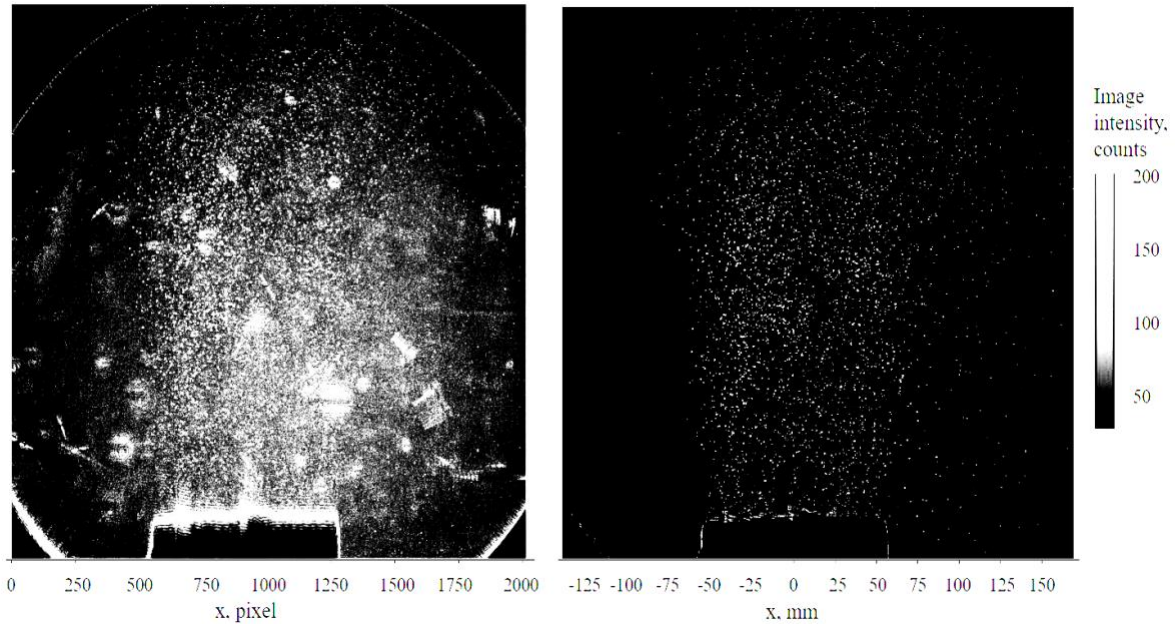

Fig. 4 Raw image (left), filtered and registered image (right) from in-line PIV recording with schlieren mirrors and light trap between the receiving mirror and the imaging lens.

The raw image data was filtered and evaluated with LaVision's DaVis software version 10.2. In order to differentiate between stationary images of dust particles, laser diffraction patterns and moving tracer particles, a temporal high-pass filter was used, which subtracted a sliding average signal over 50 images (see Fig. 4). However, many different filter options contained in the aforementioned software package yield very similar results.

To retrieve quantitative velocity data, particle tracking was applied to the filtered image data. The detected particle images had an average brightness >85 counts, with some exceptional bright particles having 500-1000 counts. The particle fit used Gaussian windows of 5x5 px. The tracking routine found about 5000 active particle tracks in each recording of an individual time step. The sample result in Fig. 7, left, depicts Lagrangian tracks consisting of 5 subsequent time steps. The color coding shows velocities between 0 m/s and 2 m/s.

The flow direction is bottom to top, and the tracks reveal turbulent structures in the instantaneous flow field. Entrainment effects introduce small velocities in the surrounding of the jet. A time-averaged result was computed over the series of 500 images by binning the PTV data to a regular grid with a window size of 64x64 px and a 75% overlap, see Fig. 5, right. Despite the short time interval, the average result reveals a more or less homogeneous velocity distribution over the jet's

cross-section. In downstream (here: upward) direction, the shear layer between the jet and the external flow thickens, whereas the maximum velocity in the jet core decreases.

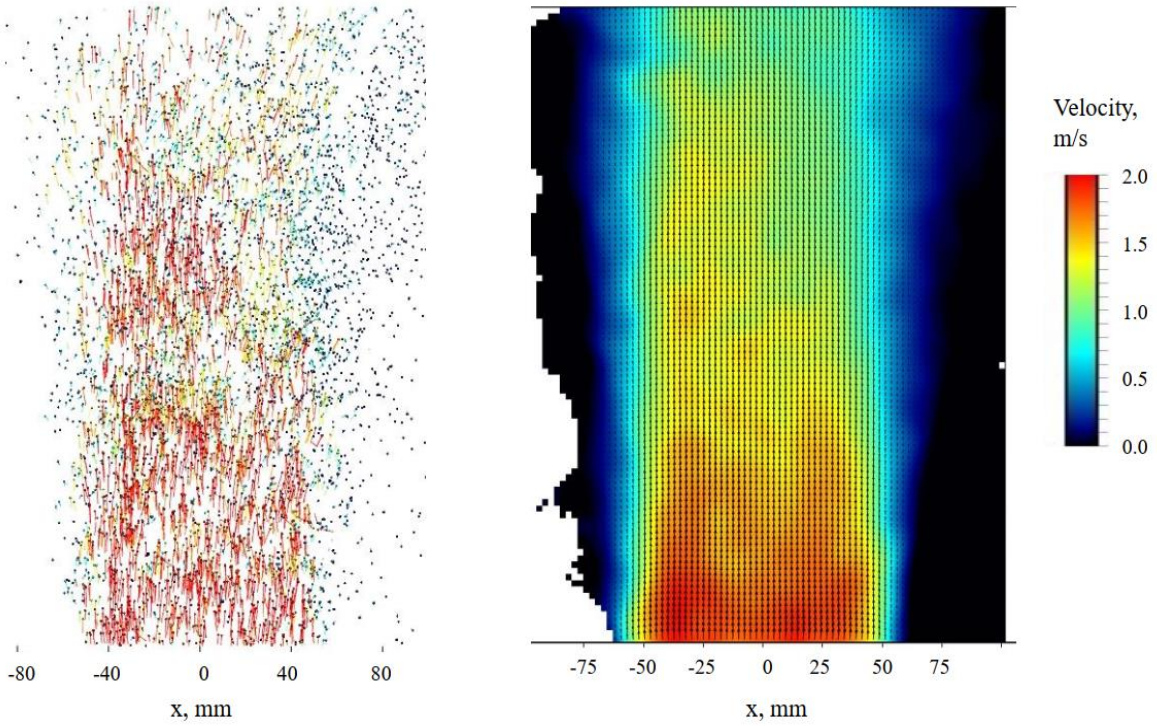

Fig. 5 Instantaneous flow field represented by particle tracks (left), and averaged flow field (right, white areas where no particle was tracked in the entire time-series), color shows velocity between 0 m/s and 2 m/s.

4. Schlieren and water droplet imaging using pulsed LED illumination

The experiment was carried out in the one-meter wind tunnel (1 MG) at DLR Göttingen, which provided a uniform flow over the measurement area with free-stream velocities between 2 m/s and 6 m/s.

Water droplets with a diameter of about D_p = 5-8 µm were provided by four small high-pressure spraying nozzles of approximately 9 mm outer diameter that were mounted in the settling chamber of the wind tunnel in order to avoid stronger turbulent disturbances in the inflow. Again, the high-speed CMOS camera (PCO.Dimax S4) with an acquisition rate of 0.5 kHz, and an image exposure time of 40 µs was used. The imaging lens was a Zeiss f = 300 mm lens set to an aperture of f# = 2.8. The image lens working distance was 4000 mm between the lens and the imaging mirror plus an additional approx. 4000 mm between the mirror and the plane of focus. To overcome the limitations of the preliminary setup, the configuration was upgraded with a double-pulsed LED

light source (Hardsoft IL-106 G) that emits green light, λ = 528 nm. The pulse duration was set to 40 µs with a pulse energy of approximately 120 µJ. A series of 1000 images was recorded within 2 seconds. For evaluation LaVision DaVis 10.2 was used with a multi pass cross-correlation method. Th initial window size was set to 64x64 px with 50 % overlap and as final window size 32x32 px with 75 % overlap was selected.

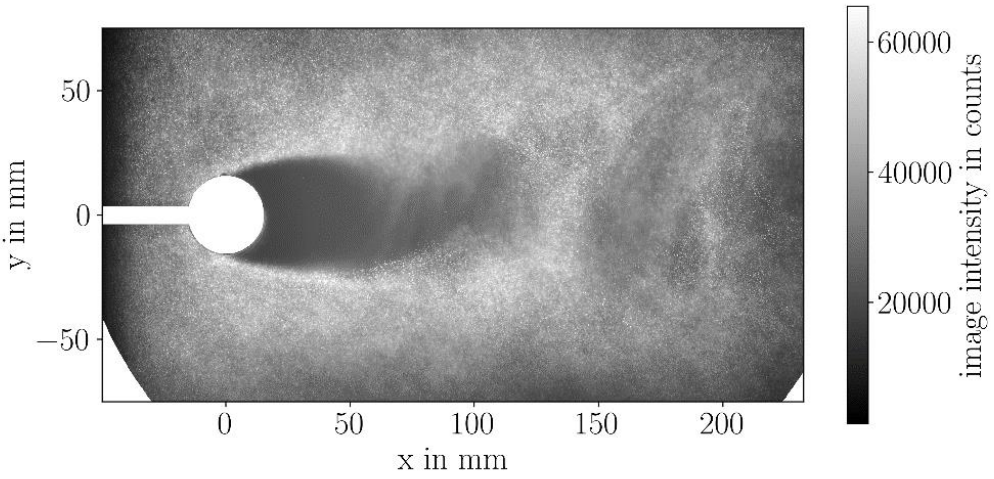

Fig. 5 Sample raw particle image (water droplets, $u_\infty = 4$ m/s).

Figure 5 shows a resulting raw image from this test with a free stream velocity of 4 m/s. The relatively large water droplets show a good contrast and don't require further processing of the raw images. However, they create a large particle void in the near wake of the cylinder. Most regions of the flow field are mapped with correlation values between 0.4 and 0.85. In the direct wake of the cylinder, however, the correlation values drop sharply or lead to uncorrelated windows. This can also be observed in the flow field resulting from the correlation, which is shown in Fig. 6. While the flow field is generally as expected, there are some false vectors in the direct wake. The average flow field over 1000 images, shown in Fig. 7 provides convincing results even in the near wake. The reason for this is that some smaller and darker water droplets sometimes occur in regions of the near wake, resulting in a correlation of parts of the near wake. The overall average fills in all gaps in the individual images.

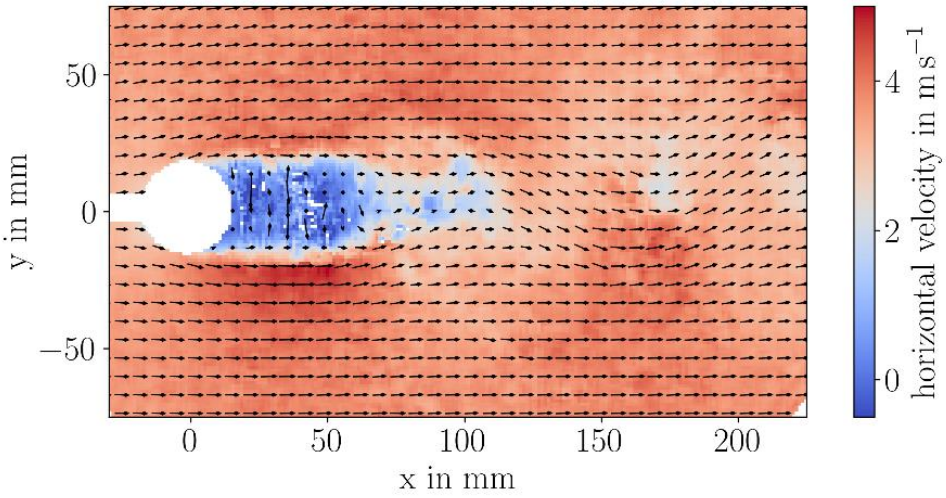

Fig. 6 Instantaneous x-velocity field ($\boldsymbol{u_\infty = 4}$ m/s).

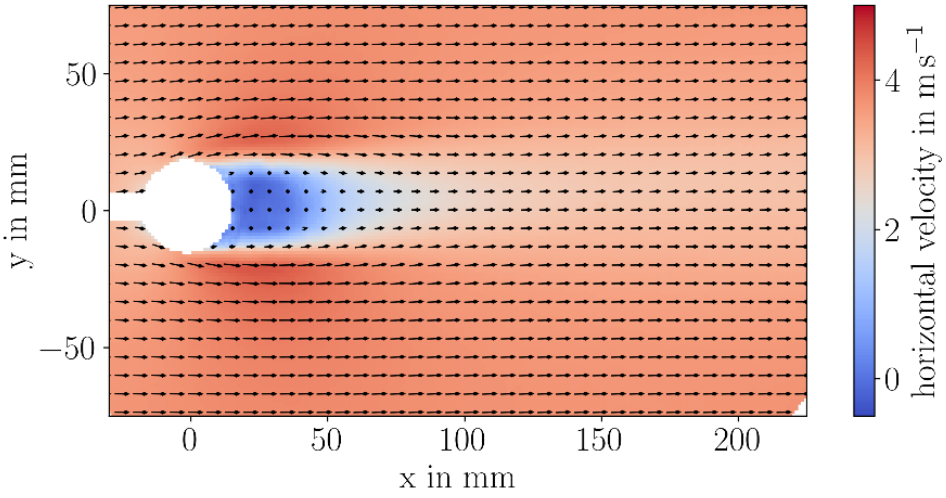

Fig. 7 Average *x-vel*ocity field ($u_\infty = 4$ m/s).

After demonstrating the feasibility of inline PIV measurements in the experimental setup with water droplets, the cylinder was heated with a hot air gun with the expectation of being able to additionally and simultaneously investigate density gradients. An example raw image of this measurement is shown in Fig. 8. Obviously, the signal strength of the schlieren image outweighs the water droplets. The overexposure in the vicinity of the cylinder excludes an evaluation of the particles, so that no meaningful flow fields can be extracted there. The average of all evaluated fields is shown in Fig. 9. As expected, the schlieren signal disturbs the PIV correlation, particularly in the wake of the cylinder edges. However, the rest of the field of view still shows reasonable velocity data. In summary, it can be stated that a simultaneous measurement of density gradients

and velocity fields was not possible due to the difference in signal strength. Nevertheless, it has been shown that both PIV and streak measurements can be carried out with the same experimental setup.

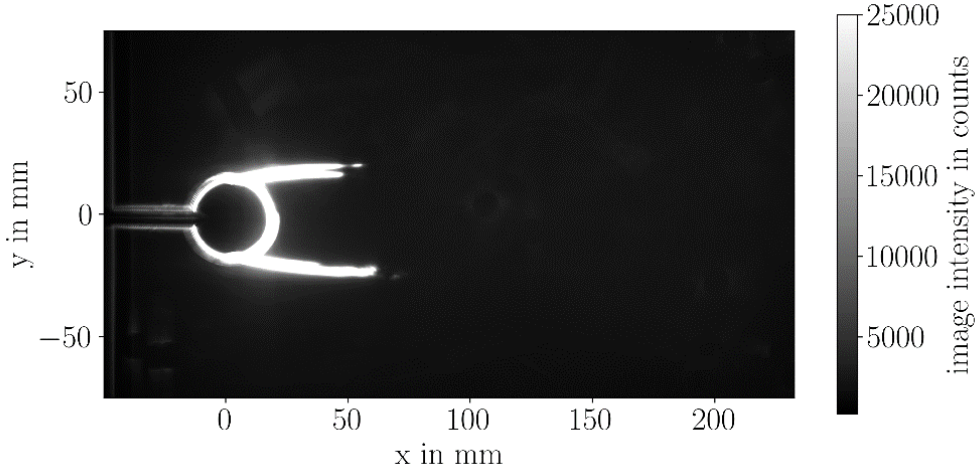

Fig. 8 Density gradients behind a heated cylinder in cross-flow visualized by the PIV/schlieren setup.

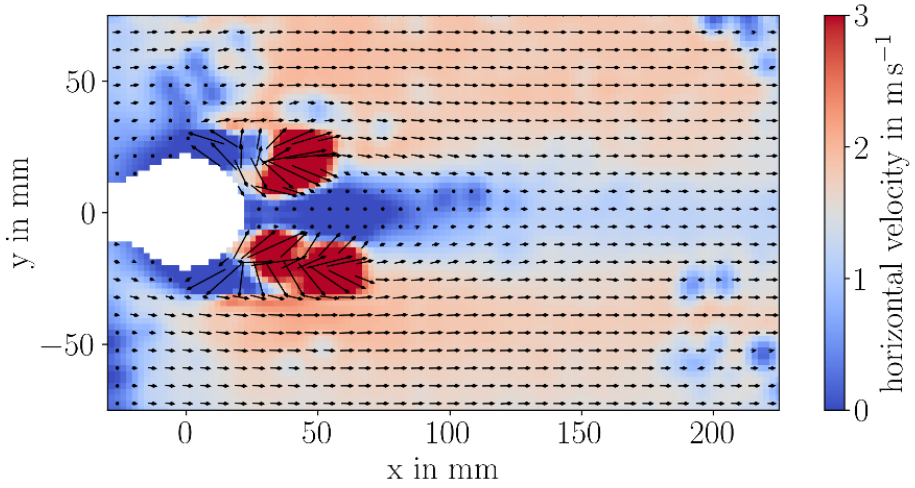

Fig. 9 Average *x-vel*ocity based on water droplet seeding with simultaneous schlieren imaging (u_∞ = 2 m/s).

5. DEHS seeding and intermittently operated CW laser

The experiment described next was again carried out in the one-meter wind tunnel (1 MG) at DLR Göttingen, but the illumination was made by a low cost cw-laser in order to allow for smaller particle diameters. Matching the frame rate of the high-speed camera, a pulse-width modulated

laser (NEJE Tool E30130, λ = 450 nm, Pcont. = 5.2 W) is triggered with pulses of 20 µs duration, thereby producing light pulses with an estimated energy of 104 µJ per pulse.
A Seika CTS-1000 seeding device provided a dense stream of di-ethylhexyl sebacate (DEHS) tracer particles approximately D_p = 1.5 µm in diameter. Due to the desire to seed just in the surrounding of the focal plane in order to avoid to many out-of-focus particles, the outlet of the seeding generator was connected to a narrow and streamlined seeding rake upstream of the cylinder test object, in order to avoid stronger turbulent disturbances in the inflow, the seeding rake was placed in the settling chamber of the wind tunnel.

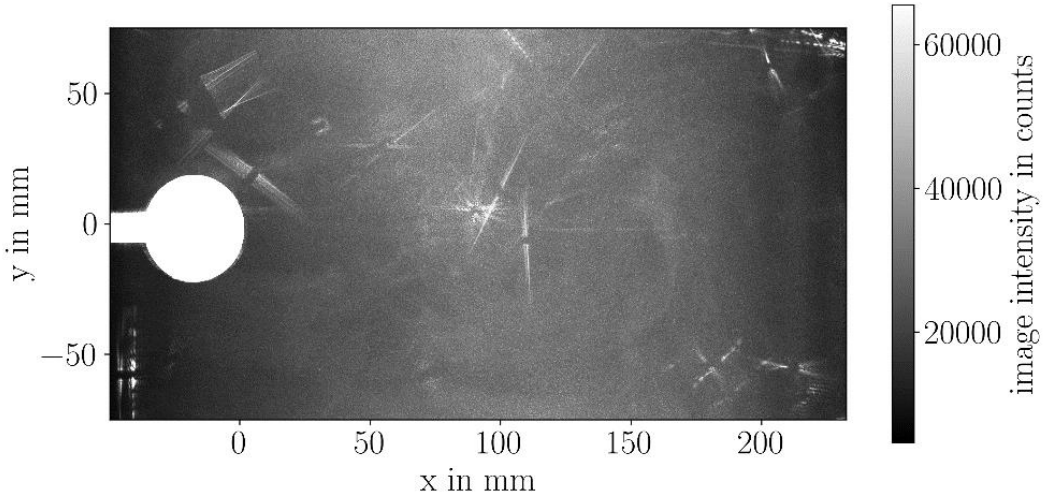

Fig. 10 Raw image of DEHS particles.

The flow direction is perpendicular to the optical axis, and a 30 mm diameter aluminum cylinder was placed at the upstream end of the measurement region to act as an obstacle to the flow. Figure 10 shows an example raw image with flow from right to left, the shear layers and the wake of the cylinder are already visible in the seeded flow. Due to imperfections on the mirror surface and a high background brightness a filter implemented in DaVis was used. The chosen filtering method involved subtracting the minimum intensity value over 3 images of each pixel and, resulting in a particle image as shown in Fig. 11, which correlates well in the PIV processing. The measurement area is 300 mm, limited by the sufficiently illuminated region. The acquired image pairs were processed with the PIV software (LaVision DaVis 10) using an adaptive iterative cross-correlation algorithm with an initial window size of 256 x 256 pixels (50% overlap) and a final window size of 96 x 96 pixels (75% overlap).

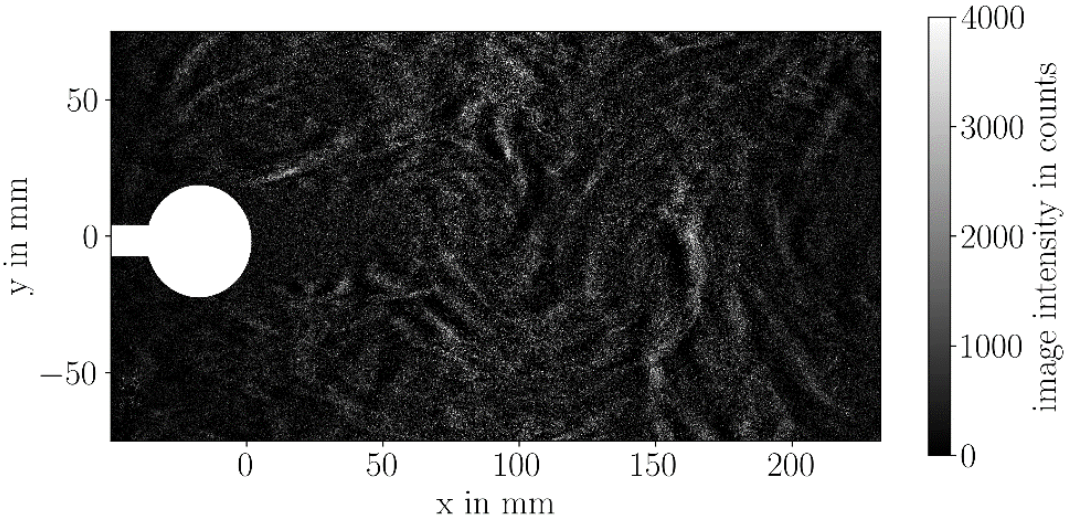

Fig. 11 Sample intensity image after the sliding background subtraction.

The average free stream velocity is approximately 6 m/s, with the turbulent wake of the cylinder clearly visible in the center of the measurement region. Note that the horizontal mounting post of the cylinder blocks the line of sight of the camera, but it is located outside the measurement region and the flow. Therefore, it does not leave a visible wake itself. The correlation value is approximately between 0 and 0.4, with the highest values in the external flow and the lowest values in the turbulent wake, respectively in loosely seeded regions.

A resulting *x*-velocity field is shown in Fig. 11. Compared to the measurements with water droplets the near wake appears to be much better resolved. The main problem with the DEHS setup was to provide for a uniformly distributed seeding in one plane. The difference in the seeding density results in loosely seeded regions that do not correlate. As a consequence, the interrogation window was increased to 96x96 pixels to ensure a sufficient number of particles in each interrogation window. Nonetheless, every recorded image still has some areas, where no correlation was possible or the correlation value is much lower than for water droplets. Figure 12 shows that this disadvantage disappears for the overall average.

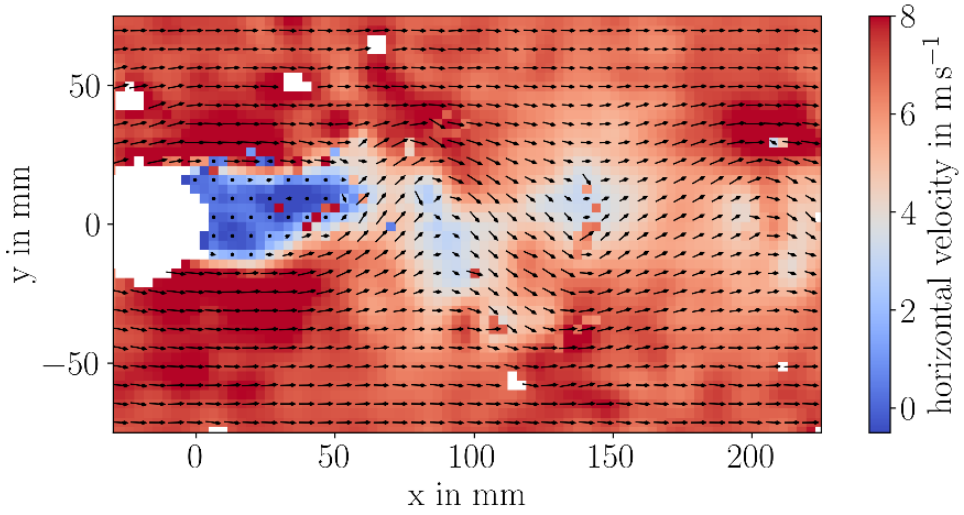

Fig. 12: Instantaneous *x-vel*ocity (DEHS, $\boldsymbol{u_\infty = 6}$ m/s).

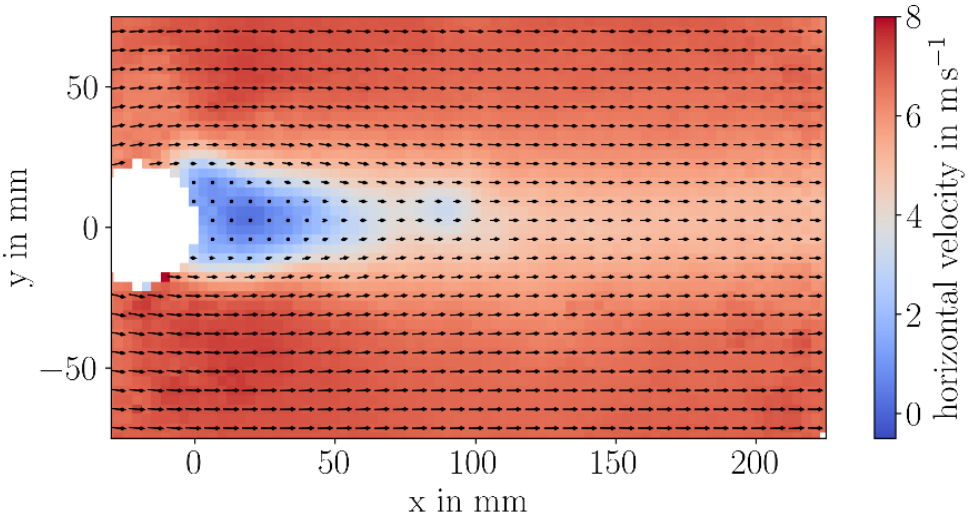

Fig. 13: Average *x*-velocity (DEHS, $\boldsymbol{u_\infty = 6}$ m/s).

5. Conclusion

We tested and described new methods of in-line PIV recording and evaluation. The in-line PIV configurations set up utilizing schlieren mirrors showed the feasibility to obtain larger fields of view of up to 0.4 m width. Simultaneous visualization of the density gradients could not be achieved, because of the high intensity levels that occurred, when the cylinder was heated. The technique worked best with high particle concentrations in the regime of the focal plane, but low particle

concentrations outside of the measurement domain. It allows a considerably increased observation area utilizing large aperture mirrors. Based on the authors' experience several results can be summarized:

- Tracer seeding within the imaging path, which are out of focus, will significantly reduce image contrast.
- Intermediate surfaces such as windows, mirrors and lenses should be kept clean and should preferably by of high quality.
- A combination of long focal length with large aperture and a considerable working distance can achieve a depth of the measurement domain in the millimeter range.
- For highly three-dimensional flows a limited depth of field requires the reduction of the separation time between both exposures to prevent loss of particle image pairing, just as in conventional PIV where the light sheet thickness defines the depth of the measurement domain.
- The in-line imaging arrangements have a relatively high background intensity level on which brighter particle images can be detected. Ideally this background is constant in time such that it can be removed through subtraction.
- The use of forward scattering has a significant influence on the required pulse energy of the light source used. Typically, sufficient illumination is achieved with about 1% of the pulse energy that would normally be used for a conventional orthogonal PIV arrangement employing a laser light sheet.

It should be noted that the present work does not cover all possible configurations, nor have all aspects of this interesting technique been fully explored. Nonetheless, it can be concluded that for some experimental setups interesting variations of the recording arrangement going along with substantial reductions in the required light power can be achieved.

Acknowledgments

The authors would like to acknowledge the help of Markus Krebs and Karsten Pfeiffer during the preparation and conduction of the experiments.

References

Adrian RJ (1991) Particle-imaging techniques for experimental fluid mechanics. Annual Review of Fluid Mechanics 23(1):261–304. https://doi. org/10.1146/annurev.fl.23.010191.001401

Bohren CF, Huffman DR (1998) Absorption and Scattering by a Sphere, John Wiley & Sons, Ltd, chap 4, pp 82–129. https://doi.org/10.1002/ 9783527618156.ch4

Raffel M, Willert CE, Scarano F, et al (2018) Particle Image Velocimetry - A Practical Guide, 3rd edn. Springer AG, Cham, Switzerland, https://doi.org/10.1007/ 978-3-319-68852-7

Raffel M, Braukmann JN, Willert CE, Giuseppini L, Wolf CC (2024) Feasibility Study of In-Line Particle Image Velocimetry, Exp. in Fluids, 65:35. https://doi.org/10.1007/s00348-024-03766-4

Naumann H, Schröder G (1992) Bauelemente der Optik - Taschenbuch der technischen Optik, 6th edn. Carl Hanser Verlag, Vienna, Austria

Schardin, H. (1934). Das Toeplersche Schlierenverfahren. VDI-Forsch. Heft, 367, 15.

Schardin H (1942) Die Schlierenverfahren und ihre Anwendungen. Ergebnisse der exakten Naturwissenschaften 20:303–439

Settles GS (2001) Schlieren and Shadowgraph Techniques, 1st edn. Springer International Publishing AG, Cham, Switzerland, https:// doi.org/10.1007/978-3-642-56640-0